




Enthalpy of Mixing of Sodium Borosilicate Glasses by DSC Analysis

Jan-Oliver Fritzsche^{1,2,*} , Christoph B. M. Groß^{2,**} , and Joachim Deubener¹ 

¹Clausthal University of Technology, Institute of Non-Metallic Materials, 38678 Clausthal-Zellerfeld, Germany

²Central Research and Development & Technical Service, SCHOTT AG, 55122 Mainz, Germany

*Correspondence: Jan-Oliver Fritzsche, jan-oliver.fritzsche@tu-clausthal.de

**Correspondence: Christoph Groß, christoph1.gross@schott.com

Abstract. An easy-to-use method to determine the enthalpy of mixing (ΔH_{mix}) from the differential scanning calorimetry (DSC) heating curve of demixed borosilicate glasses of the composition $z\text{SiO}_2$ $(1-z)(0.16\text{Na}_2\text{O} \cdot 0.84\text{B}_2\text{O}_3)$ with $z = 0.775, 0.55$ and 0.424 is presented. It is shown that ΔH_{mix} results from the area under the endothermic mixing event of the DSC heating curve, but that ΔH_{mix} can also be used to approximate the initial compositions of the boron-rich and silica-rich domains that exhibit the glass transition temperatures T_{g1} and T_{g2} of the DSC upscans.

Keywords: Enthalpy of Mixing, Borosilicate Glasses, Differential Scanning Calorimetry

1. Introduction

Sodium borosilicate glasses (NBS) possess one of the best-studied phase-separation ranges in the silica-rich corner of the $\text{Na}_2\text{O}-\text{B}_2\text{O}_3-\text{SiO}_2$ system, due to the wealth of technical glass products manufactured from this composition. The liquid phase-separation is usually detected visually as differences in the refractive indices of the liquid phases in combination with the small size of the demixed areas cause strong opalescence. However, demixing processes also cause a thermoanalytical trace, which can be read by differential thermal analysis (DTA) and differential scanning calorimetry (DSC). As early as 1972, Moynihan showed that demixed glasses exhibit two sufficiently separated glass transition endotherms when subjected to heating in a DTA [1]. Ten years later Gauthier & Gombert [2], [3] showed in the $\text{Na}_2\text{O}-\text{B}_2\text{O}_3-\text{SiO}_2-\text{GeO}_2$ system in addition two glass transitions a third thermal event in DSC measurements, which they correlated to the coexistence temperature of the glass via flanked clear-opalescence method. However, Polyakova [4],[5],[6] was the first to investigate several demixed NBS glasses and showed that this third endothermic event correlates with the opalescence temperature of the different samples. Here, the opalescence temperature is to be understood as the temperature at which the phase-separated glass reaches the upper boundary temperature of the phase separation region during heating and the opalescence visually disappears as the two liquid phases mix again. In the thermodynamic sense the last appearance of opalescence on heating corresponds to the highest conode, which is the isothermal construction line between two equilibrated binodal compositions. In contrast to DTA, DSC allows the determination of the corresponding enthalpy of mixing (ΔH_{mix}), which has often been used to study phase separation in organic binary systems [7], [8], but lacks application to inorganic liquids.

Therefore, a DSC study is performed using three NBS glasses with different compositions on the boron anomaly line ($R = 0.19 = \text{Na}_2\text{O}/\text{B}_2\text{O}_3$) (tie line of the endmembers ($0.16\text{Na}_2\text{O} \cdot 0.84\text{B}_2\text{O}_3$) – SiO_2) with the aim to gain deeper insight into the thermodynamics of phase-separation in NBS glasses. ΔH_{mix} is determined from the area of the endothermic event of the calibrated heat capacity (c_p) curve, checking for a possible kinetic limitation by using different heating rates and compared with solution calorimetric data for the mixture of the endmembers from the literature [9].

2. Experimental

2.1 Glass preparation

Three NBS glasses were prepared at SCHOTT AG (Mainz, Germany) by melt-quenching from optical grade raw materials as sources for the oxides Na_2O , B_2O_3 and SiO_2 and melted at $1300\text{ }^\circ\text{C}$ – $1500\text{ }^\circ\text{C}$ (depending on the SiO_2 content) in PtIr1 crucibles in an electric furnace with a stirrer as a 1 litre batch. After homogenisation, the glasses were cast onto a steel plate and rolled to a thickness of 8–10 mm to accelerate cooling. The chemical composition of the glasses was determined by X-ray fluorescence (PANalytical MagiX PRO, Amelo, Netherlands) and titration after DIN EN ISO 21078-1 for the B_2O_3 content. The analysed composition agreed with the planned values within the instrumental error and is summarised in Table 1. Figure 1 shows that their composition is placed under the immiscibility dome [8] and on the boron anomaly line ($1-z$) ($0.16\text{Na}_2\text{O} \cdot 0.84\text{B}_2\text{O}_3$) – $z\text{SiO}_2$ with $z = 0.775$, 0.55 and 0.424 . After cooling, the glasses were free of opalescent effects and optically homogeneous. Only the SiO_2 -rich and therefore highly viscous glass NBS1 showed a certain number of bubbles and a slight streakiness (see Figure 2 and Figure 3).

Table 1. Analysed molar oxide fractions of NBS1, NBS2 and NBS3 glasses and corresponding Na_2O -to- B_2O_3 ratio R .

Glass	$z \text{ SiO}_2$	$x \text{ Na}_2\text{O}$	$y \text{ B}_2\text{O}_3$	R	$M \text{ (g mol}^{-1}\text{)}$
NBS1	0.767	0.035	0.199	0.18	62.1
NBS2	0.55	0.072	0.378	0.19	63.8
NBS3	0.424	0.094	0.483	0.19	64.9

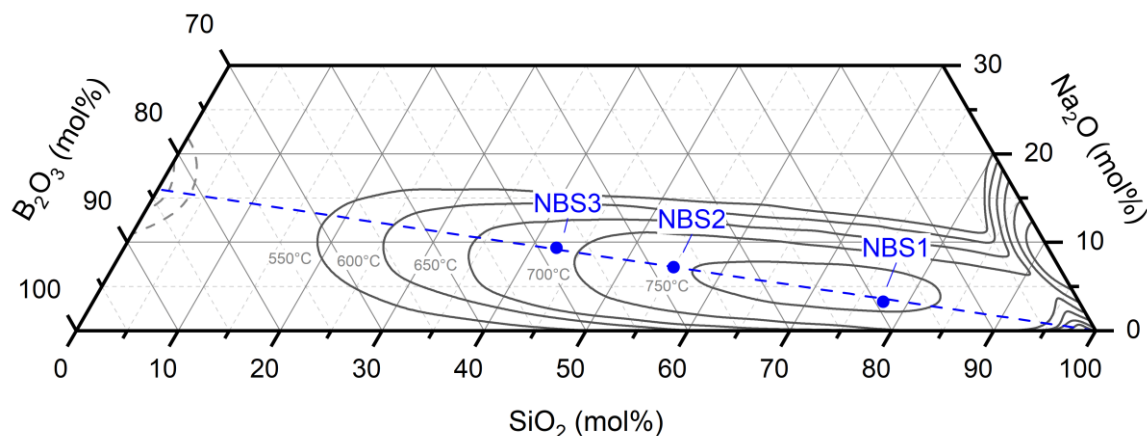


Figure 1. Na_2O -poor part of the ternary Na_2O - B_2O_3 - SiO_2 system with the three analysed NBS glasses and the isothermal lines of the immiscibility dome according to Haller et al. [10]. Boron anomaly line of Na_2O -to- B_2O_3 ratio $R = 0.2$ (blue dashed line).

2.2 Heat treatment

In order to trigger a phase separation, the three NBS glasses were thermally treated differently. A first series of glasses were exposed to a linear temperature profile ($\sim 11.5 \text{ K cm}^{-1}$) in a gradient furnace for 20 min to determine the opalescence temperature T_{opal} by subsequent visual inspection. In accordance with the results of this preliminary test, further samples of NBS1 were isothermally treated in a preheated muffle at 600 °C for 48 h and 96 h, at 700 °C for 48 h and at 800 °C for 0.5 h. For NBS 2, heat treatment was carried out at 550 °C for 96 h, 700 °C for 48 h and 770 °C for 0.5 h while for NBS3, samples were annealed at 550 °C for 48 h, at 695 °C for 3 h and at 730 °C for 0.5 h. The samples treated above the T_{opal} were taken out immediately from the hot furnace, to avoid additional phase separation from too slow cooling. The other samples were cooled down in the furnace with a cooling rate of approx. 3 K min^{-1} .

2.3 Thermal analysis

Differential scanning calorimetry (DSC 404 F1/F3 Pegasus, Netzsch, Selb, Germany) was carried out using cylindric test specimens of 4 mm diameter and 1.2 mm height ($\sim 30 \text{ mg}$) that were prepared from the untreated and treated glasses by drilling and grinding. Test specimens were heated with 10 K min^{-1} from 20 °C to 830 – 900 °C (depending on SiO_2 content) in a lidded PtRh20 crucible in an argon atmosphere (50 ml min^{-1}). Several characteristic temperatures were determined from the DSC curves. The glass transition temperatures T_{g1} and T_{g2} of the boron- and silica-rich glass domains were determined by the tangent method using the onset of the corresponding endothermic event, while the critical temperature T_c was taken at the peak of the subsequent endothermic event according to Polyakova [4]. This peak is caused by the heat consumption of the sample while it is entropically forced back into a single liquid phase. The molar enthalpy of mixing ΔH_{mix} from the standard DSC was determined *via* integration of the endothermic event using a linear function for baseline interpolation. Obtained values were multiplied with molar mass M to calculate ΔH_{mix} in kJ mol^{-1} for each glass.

For NBS2 glass only, further measurements were conducted to determine c_p using sapphire as a standard. ΔH_{mix} was determined by integration of the homogenization peak in the apparent heat capacity curve

$$\Delta H_{\text{mix}} = M \int_{T_{\text{onset}}}^{T_{\text{final}}} c_p dT \quad (1)$$

comparable to the standard DSC procedure. For removing the thermal history of the melt-quench preparation the NBS2 glass was heated and cooled with the same rates (3.33 ; 10 and 20 K min^{-1}) during c_p measurements.

2.4 Microstructure

A scanning electron microscope (SEM, LEO Gemini 1550, Zeiss, Oberkochen, Germany) in InLens mode with an operating voltage of 10 kV was used to visualise the microstructure of untreated and thermally treated glass samples. To ensure sufficient conductivity, the SEM samples were sputtered with a Pt layer of approximately 2–3 nm.

3. Results

3.1 Opalescence temperature and microstructure

Figure 2 shows the visual appearance of the glass samples after exposing them to a linear temperature profile in a gradient furnace for 20 min. The opalescence temperature T_{opal} was obtained as the temperature at which the bluish opalescence of the phase separated glass

disappears. T_{opal} decreases with decreasing z and is $\sim 745^\circ\text{C}$ for NBS1, $\sim 745^\circ\text{C}$ for NBS2 and $\sim 695^\circ\text{C}$ for NBS3.

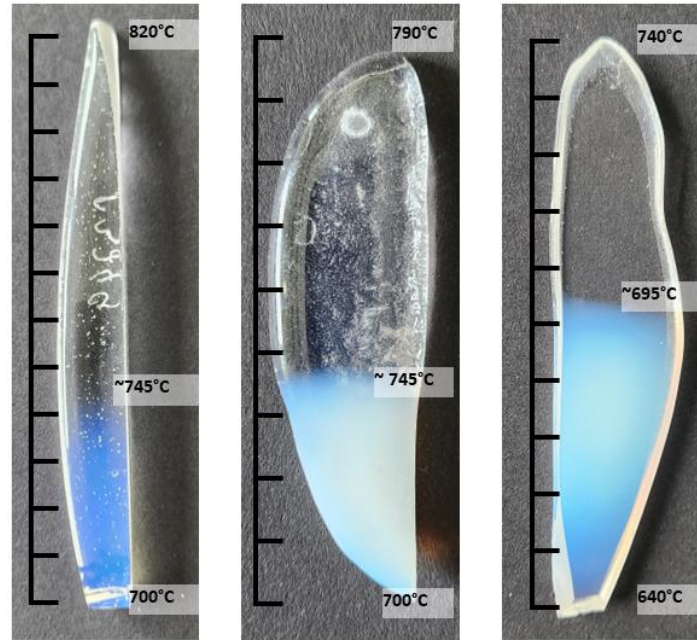


Figure 2. Opalescence temperature T_{opal} of glasses NBS1 (left), NBS2 (centre) and NBS3 (right), determined after 20 minutes of heat treatment in a furnace with a linear temperature gradient of approx. 11.5 K cm^{-1} . Upper and lower temperature (10 K steps = 0.87 cm) of the linear section in the furnace as indicated.

Figure 3 shows the microstructure along with the visual appearance of the second series of samples that were isothermally heat-treated at specific temperatures and times. The untreated glasses were transparent and transparency was maintained even when heat-treated above T_{opal} , i.e. at 800°C (NBS1), 770°C (NBS2) and 730°C (NBS3) for 0.5 h each. Opalescent glasses were obtained by heat treatment below T_{opal} , i.e. at 600°C for 48 and 98 h (NBS1), 550°C for 96 h (NBS2) and 550°C for 48 h (NBS3), while heating at 700°C for 48 h (NBS1), 700°C for 48 h (NBS2) and 695°C for 3 h (NBS3) resulted in opaque white samples. Opalescent and opaque samples showed the characteristic microstructure of demixed borosilicate glasses comprising boron-rich and silica-rich domains of either binodal or spinodal type. The domain sizes or distances ranged from the nm range for opalescent glasses, such as NBS1- 600°C -96 h, to the μm range for opaque samples, such as NBS2- 700°C -48 h.

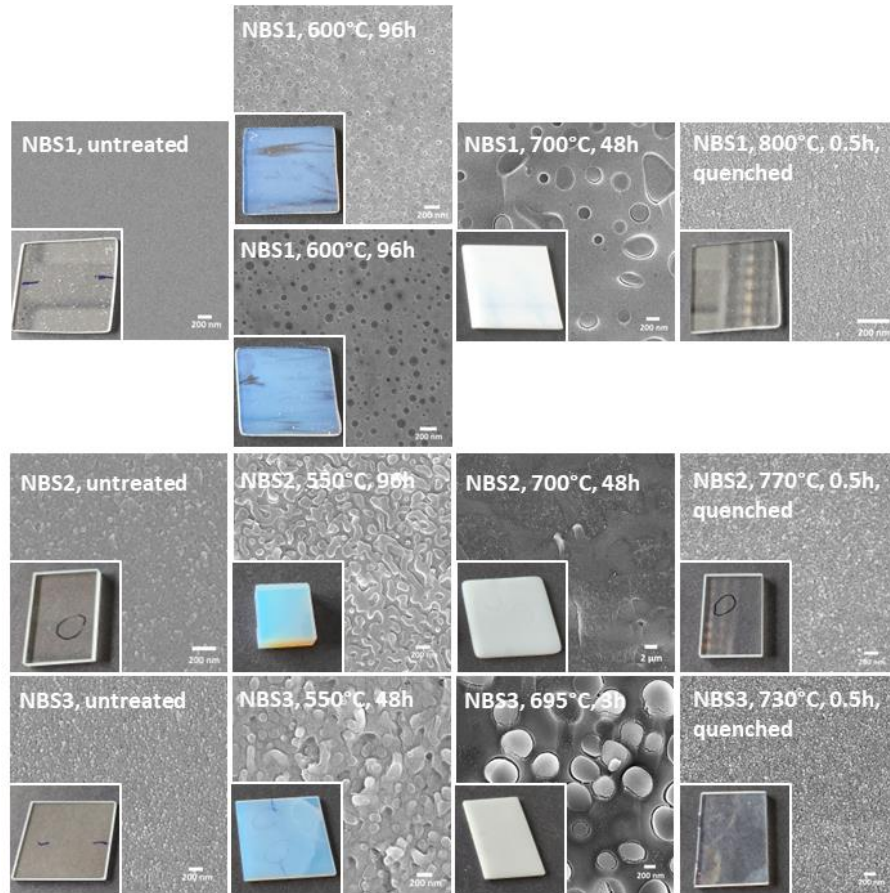


Figure 3. Microstructure (SEM images) and optical appearance (inserts) of NBS1 (top row), NBS2 (middle row) and NBS3 (bottom row) according to the specified heat treatment protocol.

3.2 Thermal analysis

Figure 4 shows DSC upscans of the preheated samples from Figure 3. As the vertical blue dashed line in Figure 4 reveals, the lower glass transition temperature T_{g1} of the boron-rich glass domains is almost constant. In contrast, the upper glass transition temperature T_{g2} of the silica-rich glass domains increases with increasing temperature/time of the previous heat treatment, more pronounced in the SiO_2 -rich NBS1 glass (green dashed lines in Figure 4). However, the lowest increase in T_{g2} is obtained for the sample pre-annealed above T_{opal} (grey curves at the bottom of Figure 4) as compared to the untreated one. The small difference indicates that quenching from the muffle used for annealing probably resulted in a slight different microstructure than cooling in the furnace (see corresponding SEM images in Figure 3). In addition, a weak dependence of the critical temperature T_c on the thermal pre-treatment becomes clear (red dashed line). Furthermore, the heat of mixing associated with the critical temperature T_c (coloured area below the peak in Figure 4) decreases slightly with decreasing silica content in the untreated starting glass from NBS1 to NBS3, while T_c itself shows only a weak dependence on the thermal pretreatment (red dashed line), except NBS1 and NBS2 at 700°C heat-treatment temperature, which might result from kinetic and secondary phase separation effects. All characteristic temperatures of the DSC measurements were listed in Table 2.

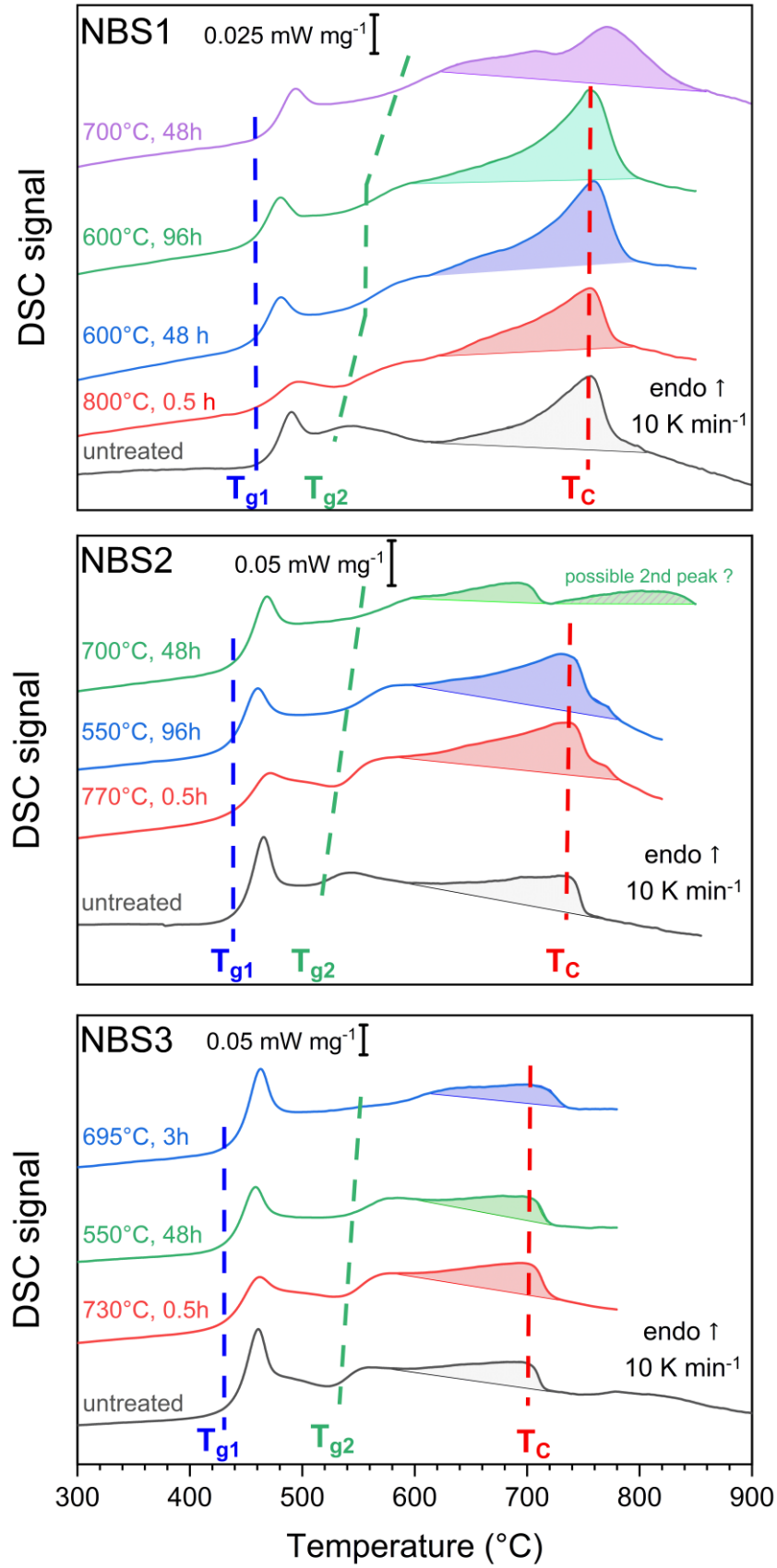


Figure 4. DSC upscans (10 K min⁻¹) of the preheated NBS1, NBS2 and NBS3 samples. Blue, green and red dashed lines highlight changes in T_{g1} (boron-rich domains), T_{g2} (silica-rich domains) and T_c of the demixed glasses with the preheating protocol.

Figure 4 also shows, as expected, that the change in specific heat flow associated with the glass transition is greater for the boron-rich domains than for the silica-rich domains and that the former increases further with decreasing z in the initial glass composition (from 0.025 mW mg⁻¹ for NBS1 to 0.05 mW mg⁻¹ for NBS3).

Table 2. Glass transition temperatures T_{g1} (boron-rich glass domains), T_{g2} (silica-rich glass domains), critical temperature of mixing T_c and enthalpy of mixing ΔH_{mix} (error $\pm 10\%$) from DSC measurements for different pre-treatments.

Glass	Pre-treatment	q (K min ⁻¹)	T_{g1} (°C)	T_{g2} (°C)	T_{onset} (°C)	T_c (°C)	T_{final} (°C)	ΔH_{mix} (kJ mol ⁻¹)
NBS1	untreated	10	468	515	619	758	799	1.0
	600 °C / 48 h	10	456	537	607	759	803	1.4
	600 °C / 96 h	10	456	539	607	756	813	1.6
	700 °C / 48 h	10	467	573	636	(780)*	840	1.1
	800 °C / 0.5 h	10	460	537	601	756	809	1.2
NBS2	untreated	10	444	512	570	735	769	1.2
	550 °C / 96 h	10	435	535	589	733	766	1.5
	700 °C / 48 h	10	443	553	597	(695) [†]	720	0.5
	770 °C / 0.5 h	10	438	534	589	736	766	1.4
NBS3	untreated	10	439	527	559	696	739	1.3
	550 °C / 48 h	10	434	538	582	701	729	1.6
	695 °C / 3 h	10	441	530	573	702	754	1.1
	730 °C / 0.5 h	10	432	538	580	700	748	1.5

*broader peak due to dissolution kinetic of ~ 500 nm droplets

[†]splitting of peak due to secondary demixing

Figure 5 shows the temperature curve of the specific heat capacity of the untreated NBS2 glass, from which the mixture enthalpy ΔH_{mix} was determined according to Eq. (1) for three different heating rates. In addition, the cooling and a second heating are also shown to illustrate the reversibility of the process. As expected, T_{g1} and T_{g2} increase as the heating rate increases, while T_c remains constant. Note that small differences in T_{g1} and T_{g2} between the first and second upscan are due to the different thermal history. While the first upscan involves a quenched glass with an unknown cooling rate, the cooling rate is identical to the heating rate in the second upscan. During the cooling the peak sharpness of the endothermic event changes, for lower cooling rates (3.33 K min⁻¹) the peak is very sharp, while for 20 K min⁻¹ it becomes flatter. From that also T_c also slightly shifts to lower temperatures with increasing cooling rate, while at heating the opposite behavior is visible. ΔH_{mix} also changes with alteration of cooling and heating rates (see Table 3).

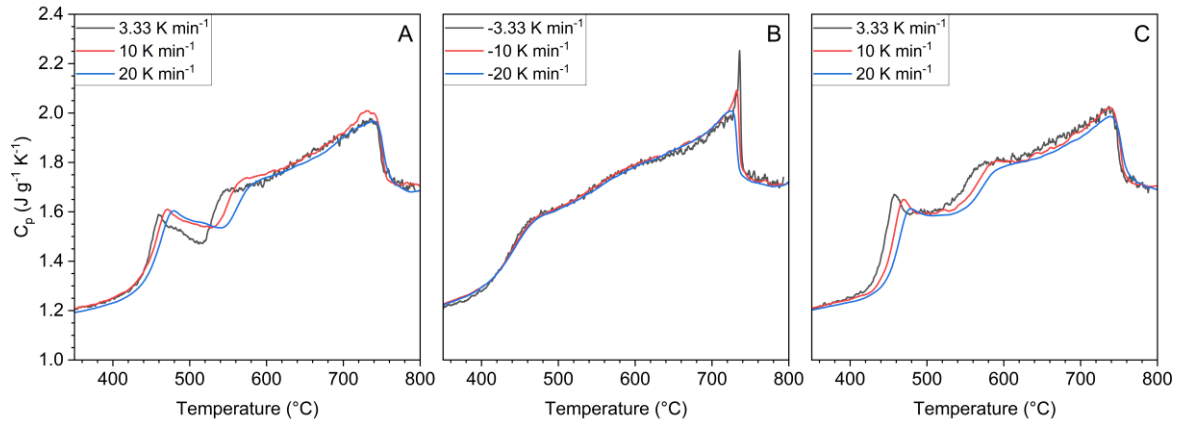


Figure 5. Specific heat capacity of NBS2 glass of the first upscan (A), subsequent downscan (B) and second upscan (C) for three different heating/cooling rates used in the DSC.

Table 3. Glass transition temperatures T_{g1} (boron-rich glass domains), T_{g2} (silica-rich glass domains), critical temperature of mixing T_c and enthalpy of mixing ΔH_{mix} (error $\pm 10\%$) of NBS2 glass from c_p measurements for different heating and cooling rates q .

Segment	q (K min ⁻¹)	T_{g1} (°C)	T_{g2} (°C)	T_{onset} (°C)	T_c (°C)	T_{final} (°C)	ΔH_{mix} (kJ mol ⁻¹)
1 st upscan	3.33	434	518	590	740	751	1.40
	10	438	537	595	735	756	1.41
	20	441	552	640	742	762	1.09
1 st downscan	-3.33	398	-	580	735	737	1.30
	-10	412	-	605	730	735	1.11
	-20	406	-	620	720	732	0.94
2 nd upscan	3.33	434	524	605	740	750	1.25
	10	442	547	600	740	757	1.28
	20	449	552	640	742	762	1.02

Figure 6 compares the ΔH_{mix} of the untreated glass with the values determined for the pretreated glass. It shows that the pre-treatment has an influence on the ΔH_{mix} in the sense that the opalescent samples treated at the lowest temperatures yielded the highest ΔH_{mix} . Among the samples pretreated at or near 700°C, NBS2 showed a lower value than the other two glasses, which emerge from the peak splitting visible in Figure 4. NBS2 and NBS3 both show comparable ΔH_{mix} to the lowest treatment temperature, which might be a hint for some segregation during the quenching, which is also visible in Figure 3. NBS1 otherwise shows a similar value as the untreated state. ΔH_{mix} of all samples were listed in Table 2.

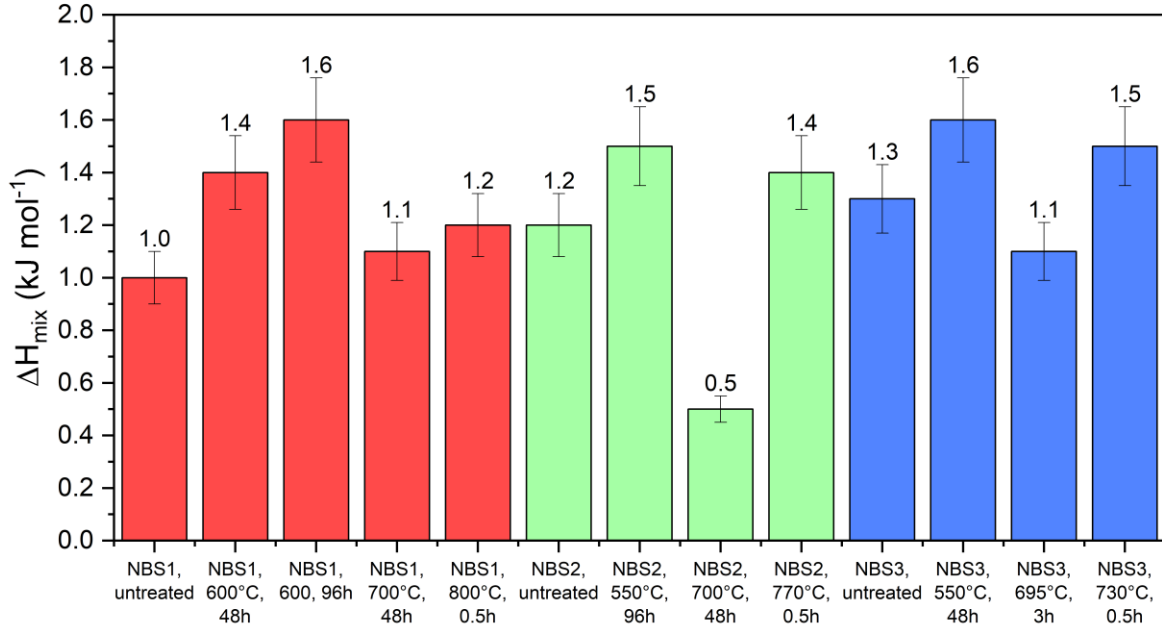


Figure 6. Enthalpy of mixing at a DSC heating rate of 10 K min⁻¹ for different thermal pre-treatments compared to untreated NBS1, NBS2 and NBS3 glass.

4. Discussion

The determination of ΔH_{mix} in the Na₂O-poor part of the Na₂O-B₂O₃-SiO₂ ternary system using thermochemical data was presented by Hervig & Navrotsky [9] for series with constant Na₂O-to-B₂O₃ ratio $R = 0, 0.25$ and 1 and by Charles & Wagstaff [11] and Pichavant [12] for $R = 0$. Assuming regular solution of the endmembers $z = 1$ (pure SiO₂ glass) and $z = 0$ (SiO₂-free glass of Na₂O/B₂O₃ ratio R) by the equation

$$\Delta H_{\text{mix}} = Lz \times (1 - z) \quad (2)$$

they revealed that the constant L is small but positive for immiscible compositions of the ternary system, with a maximum near the boron anomaly line of $R = 0.2$, for which $L = 16.7 \pm 2$ kJ mol⁻¹ can be while outside this range L is strongly negative (Part (A) of Figure 7). Part (B) of Figure 7 compares ΔH_{mix} from Eq. (2) predicted for the mixing of the endmembers of the boron anomaly line ($R = 0.2$) with ΔH_{mix} of NBS2 glass obtained from the DSC upscan for different heating rates (see Figure 5 and Table 2). Assuming a regular solution, the composition of the boron-rich and silica-rich domains mixing at T_c can be estimated as $z = 0.22$ and 0.78 (3.33 K min⁻¹), $z = 0.24$ and 0.76 (10 K min⁻¹) and $z = 0.26$ and 0.74 (20 K min⁻¹).

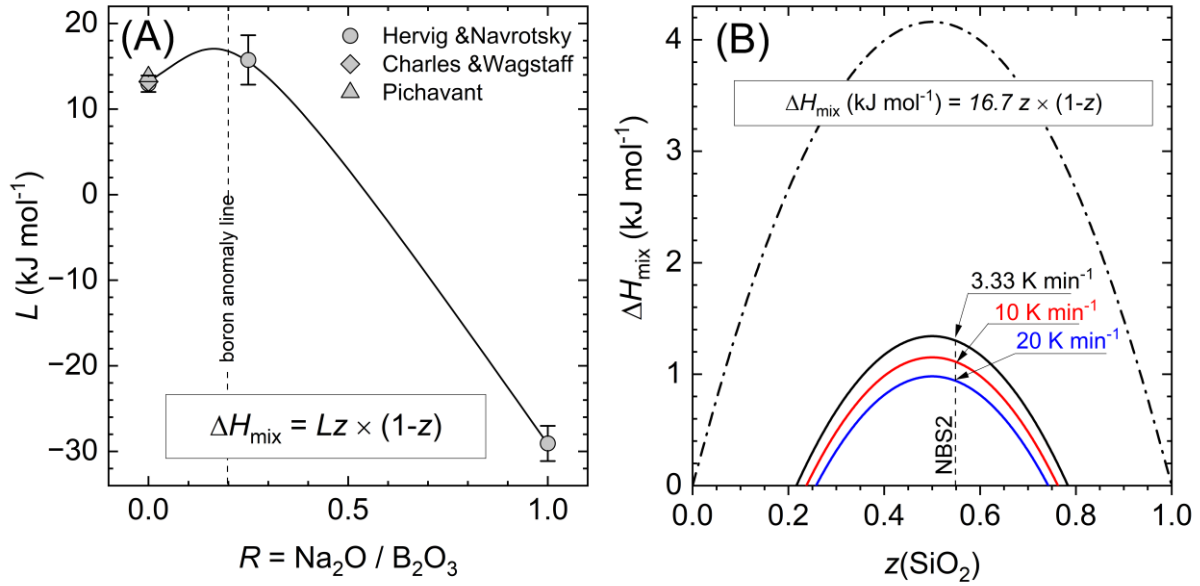


Figure 7. (A) Constant L of Eq. (2) as a function of the Na_2O -to- B_2O_3 ratio. Dashed line indicates boron anomaly with $R = 0.2$, while solid line is a visual guide. Data from Hervig & Navrotsky [9], Charles & Wagstaff [11] and Pichavant [12] (B) Enthalpy of mixing as a function of the silica fraction z for $R = 0.2$ with ΔH_{mix} values obtained from DSC measurements of untreated NBS2 glass for cooling rates of 3.33, 10 and 20 K min^{-1} .

The slight increase in ΔH_{mix} with decreasing heating rate indicates that ΔH_{mix} is probably kinetically limited. However, to test the extent to which these values are affected, the glass transition temperatures T_{g1} and T_{g2} of the boron-rich and silica-rich domains of NBS 2 glass were assigned to the compositions determined from part (B) of Figure 7 and plotted on the left side of Figure 8 together with the opalescence temperatures along the boron anomaly line ($R = 0.2$). To better visualise the corresponding calorimetric features, the heat capacity of the 2nd upscan of Figure 5 is shown again on the right-hand side of Figure 8, but in a vertical orientation to create the same temperature ordinate. With this construction, the sequence of processes that take place during the heating (for example at a rate of 3.33 K min^{-1}) of the untreated glass can be analysed. The homogeneous glass segregates during heating, so that at 444 °C (T_{g1}) boron-rich glass domains show the beginning of the glass transition (i.e. they start to relax into a liquid) and at 512 °C (T_{g2}) the silica-rich glass domains show the same characteristic. At around 600 °C the boron-rich domains reach the binodal equilibrium composition of the liquid-liquid phase separation and as the temperature increases their composition follows the binodal line. Along the binodal line, their composition becomes poorer in boron and their fraction decreases accordingly, leading to an increasing endothermic event. Note that T_{onset} , i.e. the lower limit of the integral of Eq. (1), is close to 600 °C. On the other hand, the silica-rich domains only reach the binodal line close to T_C , where the maximum of the endothermic signal is located. Above T_C , the endothermic signal drops steeply and ends at T_{final} . In the metastable immiscibility region on the left, T_C is the temperature of the limiting conode where biphasicity prevails.

The outlined process requires that the diffusive phase separation by mobile boron units already starts before T_{g1} , but that the composition in both domains remains constant during further heating, i.e. a decrease in supersaturation is prevented by a long-range diffusive exchange through the higher viscous silica-rich domains. The proximity of T_{onset} with the temperature at which the boron-rich domains meet the binodal line and the proximity of T_C and T_{final} with the temperature of the last conode speak in favour of these assumptions, but also show a delay of 10-20 K even at the lowest heating rate. The process is also supported by the results of Polyakova [6], who showed that in the sodium borosilicate system the signs of immiscibility disappear with an average temperature reduction of 50 K below the DTA-determined glass

transition temperature of the resulting single-phase glass. This implies that the lower boundary of the liquid-liquid phase separation is below T_{g1} and T_{g2} and that the phase separation evolves during heating from this lower limit to the domain compositions as indicated in *Figure 8*.

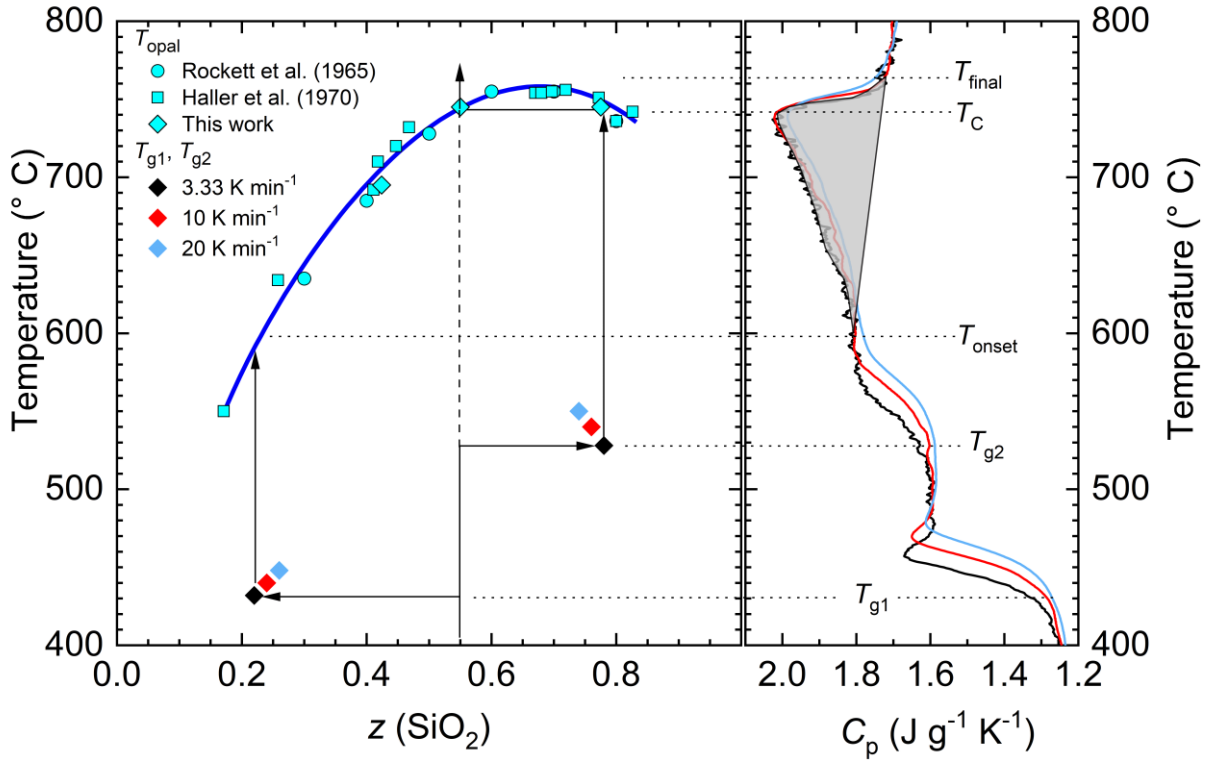


Figure 8. (Left) Immiscibility dome (binodal compositions) along the boron anomaly line ($R = 0.2$) of the $\text{Na}_2\text{O}-\text{B}_2\text{O}_3-\text{SiO}_2$ system with opalescence temperatures T_{opal} from Rockett et al. [13], Haller et al. [10] and this work (see Figure 2). Arrows indicate the compositional dependence on temperature of boron-rich (with T_{g1}) and silica-rich (with T_{g2}) domains assumed for the demixing of NBS2 glass during heating at 3.33 K min^{-1} . (Right) Specific heat capacity of NBS2 glass of the second DSC upscan (from Figure 5) with the same temperature ordinate than on the left to enable isothermal projections (dotted lines) from the DSC upscan (3.33 K min^{-1}) to the compositional join along the anomaly line.

For a higher DSC heating rate than 3.33 K min^{-1} (here 10 and 20 K min^{-1}), the initial supersaturation is greater. The corresponding compositions of the two segregated domains (determined from the decreasing ΔH_{mix} function, see Figure 7) move closer together. Conversely, for a heating rate lower than 3.33 K min^{-1} , the domain compositions would shift towards the binodal equilibrium compositions and thus make the initial supersaturation smaller. A similar pattern can also be developed for the two other glass compositions NBS1 and NBS3, where comparable initial supersaturations can be derived from the ΔH_{mix} function. Pre-annealing, on the other hand, leads to a higher ΔH_{mix} , which means that the initial compositions of the two domains are closer to the binodal equilibrium composition and there is only a slight supersaturation at T_{g1} and T_{g2} .

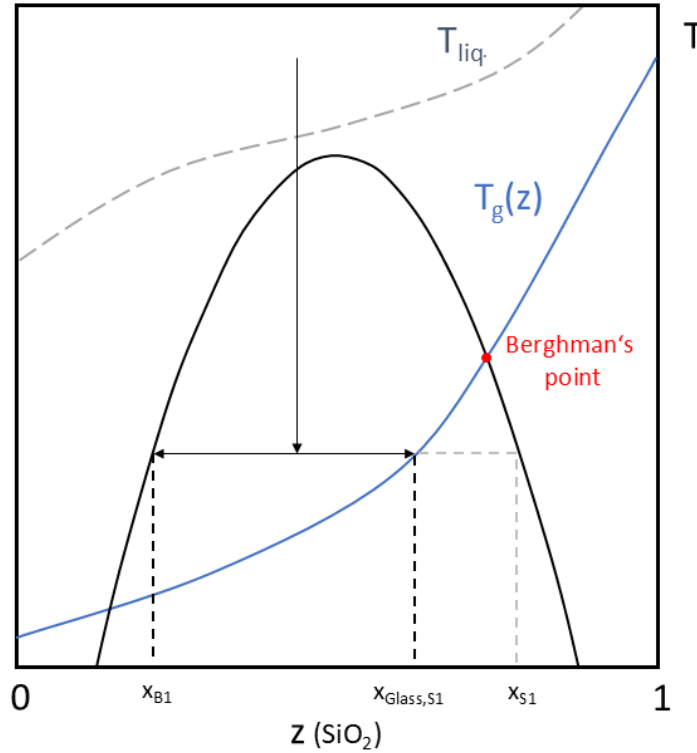


Figure 9. Schematic sketch of the immiscibility copula with differentiation between binodal and glass transition confined endmembers of phase separation, after Sappelt & Jäckle [14].

Another aspect which comes into action on the silica-rich side of the immiscibility copula is the hinderance of the high-silica phase reaching the binodal composition due to the freezing at glass transition temperature. This phenomenon is also known from polymer science, where the intersection of the glass transition and binodal line is called Berghman's point [15], [16]. Evolving from that, even at very long heat-treatment time the binodal composition will not be met for this phase, while the boron-rich phase will always reach it's binodal composition. This might also influence the magnitude of ΔH_{mix} determined with the DSC method in contrast to the drop-solution calorimetry [9].

5. Conclusions

The analysis of the demixing of borosilicate glasses using DSC shows that, in addition to the direct determination of the glass transition temperatures of boron- and silica-rich domains, their initial composition can also be estimated from the enthalpy of mixing ΔH_{mix} . The relatively small amount of ΔH_{mix} indicates that the binodal equilibrium compositions are not initially reached during heating (the demixed phases initially appear to be supersaturated on the other component). Only at the beginning of the endothermic mixing event (close to T_{onset}) does the boron-rich phase reach the equilibrium composition, while the silica-rich domains practically only reach this with the transition to the single-phase glass at T_C .

Data availability statement

The data presented within this work will be made available on request.

Author contributions

Jan-Oliver Fritzsche: Conceptualization, Formal analysis, Investigation, Visualization, Writing – review & editing; Christoph Groß: Data curation, Investigation, Resources, Validation, Writing – review & editing; Joachim Deubener: Formal analysis, Supervision, Visualization, Writing – original draft

Competing interests

The authors declare that they have no competing interests.

Acknowledgement

The authors thanks G. Kissl and P. Keil of SCHOTT AG for melting the three glasses and P. Höhn for acquisition the SEM images.

References

- [1] C. T. Moynihan, P. B. Macedo, I. D. Aggarwal, and U. E. Schnaus, “Direct observation of the double glass transition in a phase-separated glass”, *J. Non-Cryst. Solids*, vol. 6, pp. 322–328, 1971, doi: [https://doi.org/10.1016/0022-3093\(71\)90023-8](https://doi.org/10.1016/0022-3093(71)90023-8).
- [2] F. Gauthier and J. Gombert, Evolution of microstructure in a glass of the system Na₂O-B₂O₃-GeO₂-SiO₂, *Journal of Non-Crystalline Solids* 49 (1982) 157–163. [https://doi.org/10.1016/0022-3093\(82\)90114-4](https://doi.org/10.1016/0022-3093(82)90114-4).
- [3] F. Gauthier and C. Lapeyre, J. Gombert, BEHAVIOUR OF GERMANIUM IN PHASE SEPARABLE GLASSES OF THE SYSTEM Na₂O - B₂O₃ - GeO₂ - SiO₂, *J. Phys. Colloques* 43 (1982) C9-253-C9-256. <https://doi.org/10.1051/jphyscol:1982946>.
- [4] I. G. Polyakova, “Specific features of metastable immiscibility in the Na₂O-B₂O₃-SiO₂ system according to differential thermal analysis data”, *Glass Phys. Chem.*, vol. 20, pp. 386–391, 1994
- [5] I. G. Polyakova, “The regularities of metastable immiscibility in the Na₂O-B₂O₃-SiO₂ system: lower- and upper-temperature boundaries”, *Glass Phys. Chem.*, vol. 23, pp. 45–57, 1997
- [6] I.G. Polyakova, Phase equilibria in alkali borosilicate systems: facts and fictions, *Phys. Chem. Glasses: Eur. J. Glass Sci. Technol. B* 61 (2020) 131–143. <https://doi.org/10.13036/17533562.61.4.Polyakova>.
- [7] J. Arnauts, R. De Cooman, P. Vandeweerdt, R. Koningsveld, and H. Berghmans, “Calorimetric analysis of liquid-liquid phase separation” *Thermochim. Acta* vol. 238, pp. 1–16, 1994, [https://doi.org/10.1016/S0040-6031\(94\)85204-9](https://doi.org/10.1016/S0040-6031(94)85204-9).
- [8] W. Tu, Y. Wang, X. Li, P. Zhang, Y. Tian, S. Jin, and L.-M. Wang, “Unveiling the dependence of glass transitions on mixing thermodynamics in miscible systems”, *Sci. Rep.*, vol. 5, art. No. 8500, 2015, doi: <https://doi.org/10.1038/srep08500>.
- [9] R. I. Hervig and A. Navrotsky, “Thermochemistry of sodium borosilicate glasses”, *J. Am. Ceram. Soc.*, vol. 68, pp. 314–319, doi: <https://doi.org/10.1111/j.1151-2916.1985.tb15232.x>.
- [10] W. Haller, D. H. Blackburn, F. E. Wagstaff, and R. J. Charles, “Metastable immiscibility surface in the system Na₂O-B₂O₃-SiO₂”, *J. Am. Ceram. Soc.*, vol. 53, pp. 34–39, 1970, <https://doi.org/10.1111/j.1151-2916.1970.tb11995.x>.
- [11] R. J. Charles and F. E. Wagstaff, “Metastable immiscibility in the B₂O₃-SiO₂ system”, *J. Am. Ceram. Soc.*, vol. 51 pp.16–20, 1968, <https://doi.org/10.1111/j.1151-2916.1968.tb11820.x>.
- [12] M. Pichavant, “A study of the system SiO₂-B₂O₃ at 1 kbar. The phase diagram and a thermodynamic Interpretation” (in Fr.), *Bull. Mineral.*, vol. 101, pp. 498–502, 1978, <https://doi.org/10.3406/bulmi.1978.7219>.

- [13] T. J. Rockett, W. R. Foster and R. G. Ferguson Jr., “Metastable liquid immiscibility in the system silica-sodium tetraborate”, *J. Am Ceram. Soc.*, vol. 48, pp. 329–331, 1965, <https://doi.org/10.1111/j.1151-2916.1965.tb14752.x>.
- [14] D. Sappelt, J. Jäckle, Computer simulation study of phase separation in a binary mixture with a glass-forming component, *Physica A: Statistical Mechanics and Its Applications* 240 (1997) 453–479. [https://doi.org/10.1016/S0378-4371\(97\)00048-4](https://doi.org/10.1016/S0378-4371(97)00048-4).
- [15] P.C. van der Heijden, A DSC-study on the demixing of binary polymer solutions, Universiteit Twente, Enschede, Netherlands, 2001.
- [16] L.H. Sperling, *Introduction to Physical Polymer Science*, John Wiley & Sons, Ltd, 2005. <https://doi.org/10.1002/0471757128>